Efficient chip counting system with a modified scanner

Tzong-Sheng Lee
Jin-Shown Shie
National Chiao Tung University
Institute of Electro-Optical Engineering
Hsinchu, Taiwan
E-mail: 850374@hq.itri.org.tw

Abstract. A low-cost imaging system capable of recognizing and counting semiconductor good dice is designed and is proven experimentally to be effective. The system utilizes a commercial scanner with the least modification of its inner optics by a beamsplitter-insertion method. Patterns on specular die surfaces therefore can be grabbed clearly, which results in the marks on defective dice being distinguishable. Also, a mask algorithm is developed to count the good dice on an adhesive tape, according to the gray-level histogram and the converted binary picture of the scanned image. The built-in software associated with the scanner, which is reliable and user-friendly, can also be incorporated into the designated algorithm without paying an additional price for system development.
[S0091-3286(98)01409-3]

Subject terms: optical counting; scanner; semiconductor dice.

Paper 17127 received Dec. 12, 1997; revised manuscript received Mar. 24, 1998; accepted for publication Mar. 24, 1998.

1 Introduction

In the final stage of production of semiconductor devices, a wafer containing a certain kind of device is subjected to dicing, expanding (on adhesive tape), defect inspection, and ink-marking, and subsequently the number of good dice, or chips, on the sawed wafer must be counted accurately. As millions of different discrete chips, such as LEDs, photodiodes, and transistors, are produced daily in a regular foundry, however, a rapid and accurate counting system is indispensable to productivity and to avoid the possibility of future disputes over the quantity delivered to buyers.

During the packaging process, all of the dice of a sawed wafer must be kept on an adhesive tape mat, without regard to the good or ink-marked defective dice, because the cost for picking out the defective dice can be avoided, and an otherwise blank zone appears on a defective cluster area, as that shown in Fig. 4(b) (in Sec. 2) and described later. This blank zone leads a die-bonding machine to misjudge it as the edge of a wafer and the useful dice left behind on the same row will be lost. For this reason, any chip counting system must be designed to have the ability to identify the ink mark on a die surface.

Noncontact optical methods are generally adopted to acquire the graphic image of die surfaces for recognition.[1] Although it is not difficult to design such an optical system to do the job, the cost of such systems is substantial. Currently, a fully custom-designed system for such a chip counting application costs over $30,000. Normally, in a discrete device foundry, many kinds of devices are produced, each in quantities of millions daily. Therefore many counting systems are required. Reducing the investment in die counting systems therefore becomes necessary.

In the following, we describe an economical optical imaging system with an effective die counting algorithm to meet the demands of discrete device foundries. This system costs only about $1500 in U.S. dollars, much less than a commercial system.

2 Imaging System

An optical system designed for counting semiconductor dice should have the ability to identify unmistakably the ink mark on a die surface. There are many illuminating techniques to enhance image features.[2,3] However, the mirror-like semiconductor surface generally causes specular reflection. As a result, any slant illumination cannot pick up the surface characteristics of an inspected die clearly, therefore vertical incident lighting must be used instead. In many machine-vision applications, CCD cameras associated with illuminators and frame grabbers, as depicted in Fig. 1, have been used to capture images. But present-day low-cost CCD cameras do not have the resolution to recognize the detailed features of an entire wafer in one image frame. In our case, this means that the clearance between neighboring dice as well as the ink marks on die surfaces should be distinguishable. This problem cannot be solved using an expensive high-resolution CCD camera if cost factors are taken into consideration.

A linear image sensor that scans a moving object laterally produces a 2-D image.[4] Commercial low-cost scanners were designed to generate this kind of function and could be used to serve our purpose. Figure 2 shows the functional geometry of such a scanner. A wafer on the glass desk is scanned in the same way as ordinary documents are processed. Current low-cost commercial scanners, having an *A*4 size desk area, can accommodate wafers up to 8 in. in diameter and provide high image resolution of 600 dpi, which is enough to print out an entire wafer with the information for die clearance and the ink marks preserved. As depicted in Fig. 2, however, the light of a scanner is incident to the object surface at a slant (ray *c*), which does not

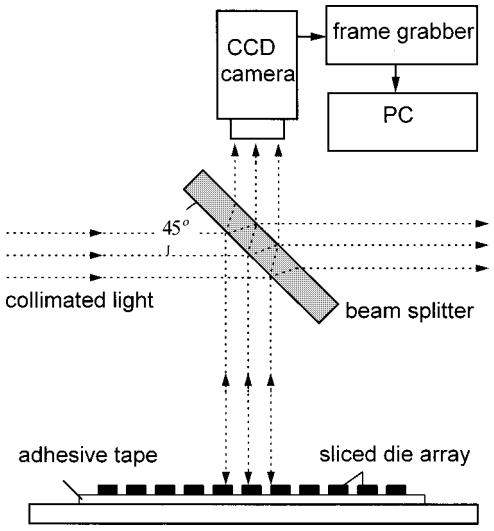

Fig. 1 Concept of recognizing the surface feature of a mirror-like chip with a traditional CCD camera by vertical lighting.

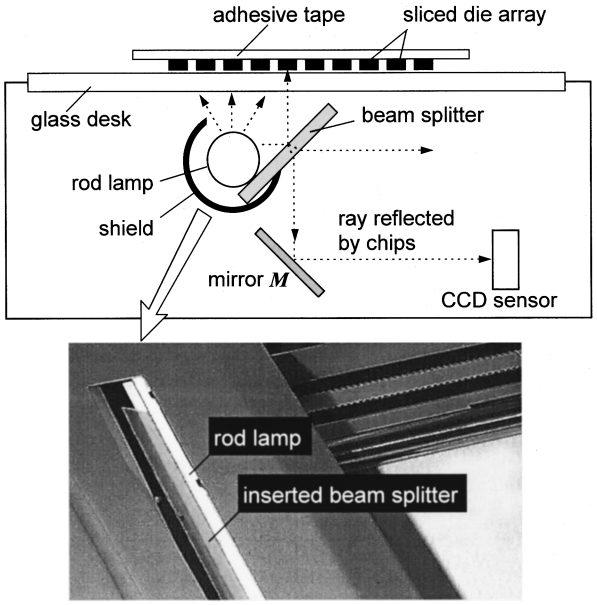

Fig. 3 Optical structure of the beamsplitter-insertion method for the modified scanner.

enable the specularly reflected light (ray *e*) from the mirror-flat chip surface to reach the CCD sensor (ray *d*) using the existing optical geometry. This is unlike the diffusive surface of paper, where there is always a fraction of light reflected along the optical path to the CCD (ray *a*). Therefore the quality of chip features obtained with the built-in optical structure of the present scanners without modification is always poor. This seriously reduces the accuracy of the count.

There are at least three ways to overcome this problem. The first method is to make the object surface translucent, so that any reflected light will be diffused, no matter from which direction the illumination comes. This diffusion can be achieved either by roughing the surface of the desk glass by sandblasting or by placing semitransparent drafting paper on the glass surface, as shown in Fig. 2. However, these techniques produce fuzzy images with poor resolution. Additionally, placing a chip face down on a rough surface can easily damage it by scratching or dust contamination. The second method is to adjust the reflecting mirror *M* in Fig. 2 from position 1 to position 2, so that the specular reflection

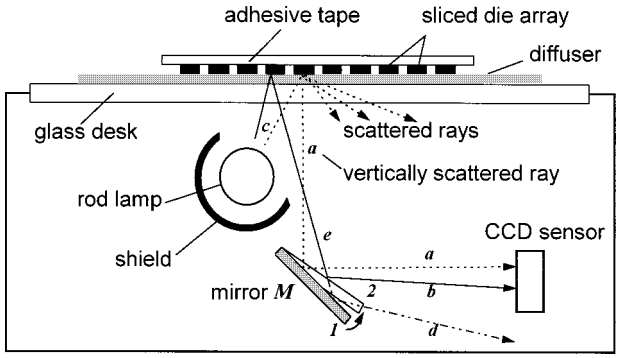

Fig. 2 Two methods of grabbing high-fidelity chip images. One method uses a diffusive window in front of the object. The light from chips is partially received by the CCD sensor (ray *a*) due to the diffusive scattering. In the other method, the mirror *M* is adjusted to a proper position 2 for correct optical path (ray *b*).

to the sensor can be achieved optically using a fraction of the lamp light, as shown by rays *c*, *e*, and *b*. The images obtained generally have good quality for our purpose, but in practice, implementation of the precise optical alignment is difficult. One must trace back to the original machine drawing, which is usually not provided by the manufacturer for small-quantity orders. The third method is to place an optical beamsplitter at a 45-deg inclination with respect to the desk surface in front of mirror *M*, as shown in Fig. 3. Note that the fraction of light emitted horizontally from the fluorescent rod lamp is partially upward reflected at the beamsplitter and is then directed perpendicular to the sample surface. This arrangement enables the sensor to receive the optical image of the sampled dice unambiguously. Notice also that due to the wide-angle light field, precise 45-deg alignment is not necessary. The insertion loss by the beamsplitter, or even just by a piece of glass, is tolerable to the minimal requirement for light intensity in this study. One can also quickly adjust the angle of the beamsplitter by testing the resultant images. This modified structure of a commercial scanner is very simple to implement. Therefore the beamsplitter-insertion method was chosen for our study. Figures 4(a) and 4(b) show two distinctly different features of a wafer taken before and after the modification.

In most automatic inspection systems, producing binary representations is generally an initial step immediately after scanning to reduce the processing load and image data.[5] Figure 5(a) illustrates part of the typical GaAsP LED image taken using the beamsplitter-insertion method. The sampled binary image, as shown in Fig. 5(c), is quite clear with a chosen threshold value indicated in the normalized histogram of Fig. 5(b). Note that in Fig. 5(a) the relatively large size of the ink marks on the small defective LED dice (10×10 mil^2) have caused them to nearly blacken and appear empty in this picture. Figures 6(a) and 6(b) show the image and the normalized histogram of a photodiode of much larger size (120×120 mil^2). The highest peak *h* in

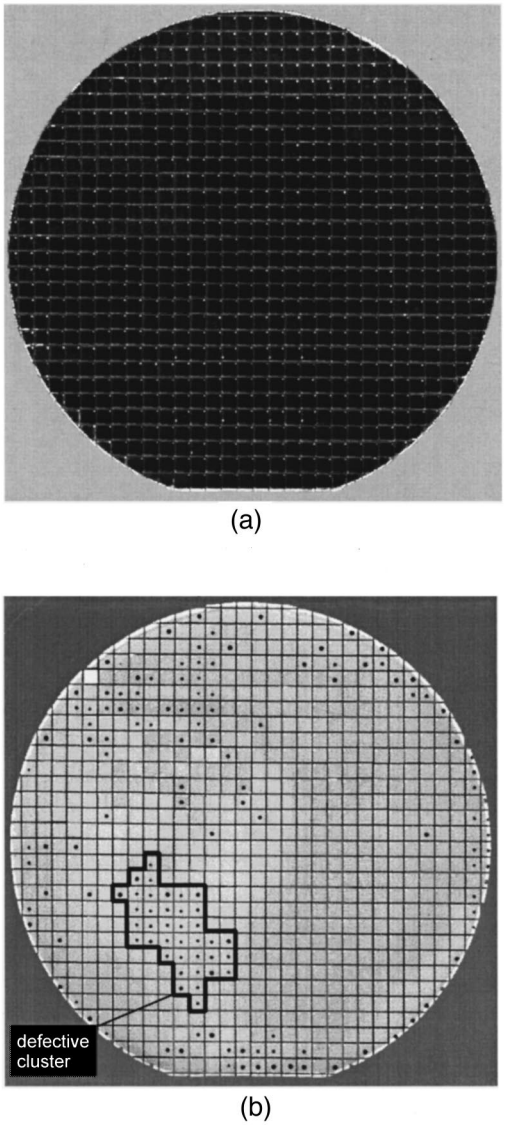

Fig. 4 Chip array image taken (a) before and (b) after beamsplitter insertion. Notice that the ink marks in the former are not observable.

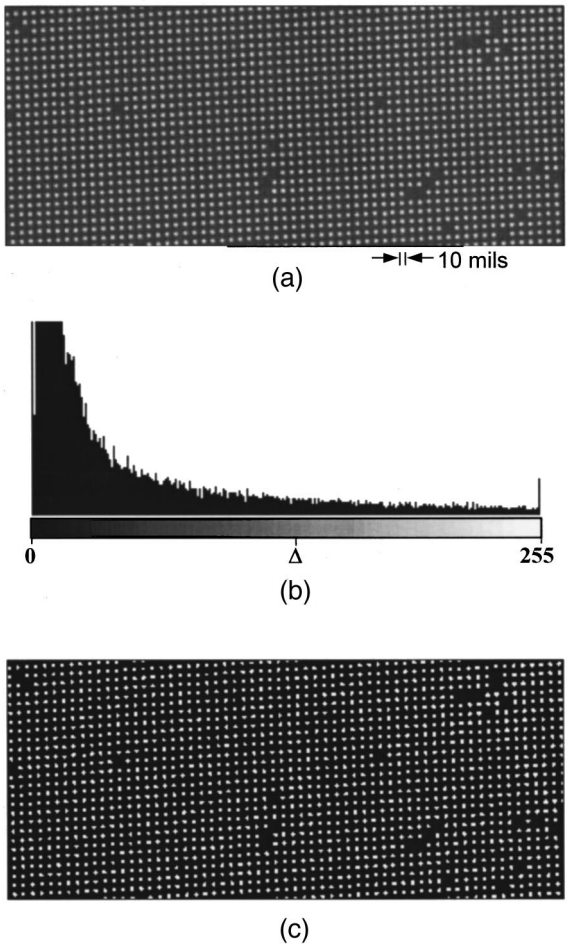

Fig. 5 Image information of a GaAsP LED chip array on an adhesive tape: (a) as grabbed by the modified scanner, (b) normalized gray-level histogram, and (c) binary image with a chosen threshold level (Δ).

Fig. 6(b) represents the brightest zone on the die surface. The second peak *m* stands for the smaller ink area of the lowest intensity, as judged from Fig. 6(a). The third peak *l* is the clearance area. The binary representation is shown in Fig. 6(c), where the ink dots on the defective dice are unambiguously clear. Note that between peaks *h* and *l* is a wide range for choosing a binary threshold, while this range is narrower for LED chips due to the lower surface reflectance of different die materials. Nevertheless, a certain range for the threshold level is selectable for each die type and no adjustment is required between different scan operations. Hence we can conclude that the binary threshold level can always be set at a constant value for all chip types. Developing an autothresholding rule is not necessary so that the operation and processing of chip counting using this system are greatly simplified. This is evidenced by the experimental data described in the following sections.

3 Counting Algorithm

Speed and accuracy are the two most important factors in testing the effectiveness of a die counting algorithm. A good algorithm should effectively utilize a device feature to optimize its performance in addition to the binary enhancement with a gray-level histogram. For a processed wafer, sliced or not, the dice are always arranged in array geometry with nearly identical unit cells,[6] such as that shown in Figs. 5 and 6. The periodicity can be useful to our purpose. An algorithm called the mask method that emphasizes utilization of this special feature was developed to identify only the good dice in a tested wafer.

The first step in identification is to take an image conversion of a sample. The scanner is set to binary scan mode with a preset gray-level threshold obtained from calibration. Then the scanned image is converted into its reverse tone and saved in the PC extended memory. To maximize the counting speed, the scanning should occur with the lowest resolution permitted by the tested chip feature. This means that the pixels of the array clearance P_c and those of the die dimension P_d must satisfy the conditions

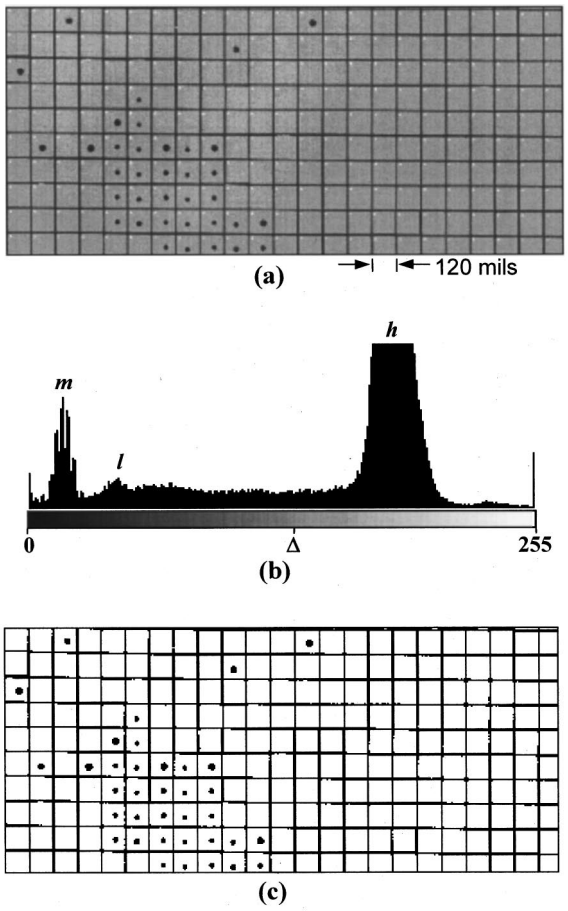

Fig. 6 Image information for a photodiode chip array on an adhesive tape.

$$P_c = \frac{Rl_c}{1000} \geqslant 1 \quad \text{(pixels)}, \quad \text{if } l_c \leqslant l_d,$$
$$P_d = \frac{Rl_d}{1000} \geqslant 1 \quad \text{(pixels)}, \quad \text{if } l_c \geqslant l_d. \tag{1}$$

Here R is the image resolution in dots per inch, and l_c and l_d are the lengths of the clearance and the die edge in mils, respectively. The conditions ensure that all die images will exist and be separate from each other after the conversion step.

A mask matrix with all of its elements in status 1 (bright) is then defined. However, the mask size should be small enough to not touch the clearance grid of a tested array of binary representation. Also, it must be large enough to be able to contain sufficient ink pixels (status 1) for identification.

A reasonable condition for the mask size is to restrict its horizontal dimension M_x in the range of

$$\tfrac{1}{2} P_d \sin 45 \text{ deg} < M_x < P_d \sin 45 \text{ deg} \quad \text{(pixels)}, \tag{2}$$

for possible maximal array tilting (45 deg) with respect to the scan direction. Since an ink mark is located close to a die center [Fig. 4(b)], this defined mask will positively cover enough ink pixels for identification. To include dice of a rectangular shape in general, the vertical dimension of the mask M_y is set relative to M_x by the die edge ratio. However, if an array can be positioned by an automatic handling machine to guarantee a small tilt, then the mask can be increased to a size slightly less than that of the test chip so that the counting can be more efficient.

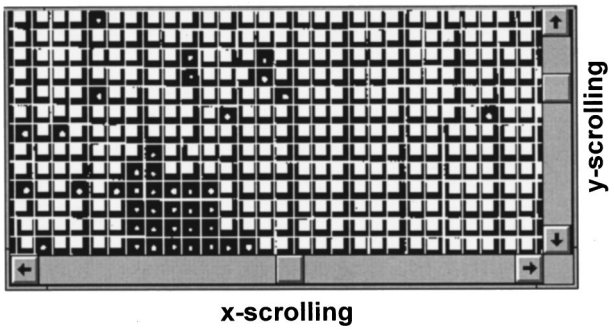

Fig. 7 Illustration of counted result displayed on screen.

After the mask is defined, it is applied to a raster scan of the binary die image. At each location that the mask is ANDed with the field it covers, the bright pixels in it can be checked. If the number of bright pixels that belong either to the ink mark or the clearance are smaller than a tolerable threshold pixel number, then a good die is possibly located around the address, and we designate it a counted mask. Otherwise, the result is simply omitted and the scan is continued for the next AND operation. A nonzero threshold value is permitted to tolerate the possibility of dust contamination on a die surface or that the grid was touched by the mask. In this paper, the threshold is 2 pixels, which means two dust particles of ~ 42 μm size for a 600-dpi image are allowed on each die, whereas an ink mark has ~ 100 pixels on average. We thus understand that an even larger threshold can be used.

A ''counted'' flag is set if it is a counted mask. To prevent repetitive counts occurring on the same die due to small mask size or its movement, however, a rectangular aperture that moves with the mask is defined with an area of $A_x \times A_y$, which is barely smaller than the unit-cell area of the array. This means that, in each dimension, the edge length is 1 pixel less than the array period, or $P_c + P_d - 1$. A count is effective only when there is no other count in the same aperture field.

The horizontal step of the mask movement S_x is set to the array period of $P_c + P_d$ if a count is assured. Otherwise, step-by-step movement of the mask with the clearance P_c is adopted. For a vertical scan, the jump step S_y is affected by the vertical die dimension M_y and the array tilt angle. A 1-pixel jump of S_y is used in this paper to have a reliable count covering any tilt. However, the operating speed can be faster if tilting can be avoided so that a larger vertical jump can be used.

Figure 7 shows an illustration of the screen after a count cycle is completed. The screen can be scrolled after counting is finished to compensate for overfilling the scope by the entire field of wafer information. This enables the user to browse quickly for the missed dice in the previous cycle.

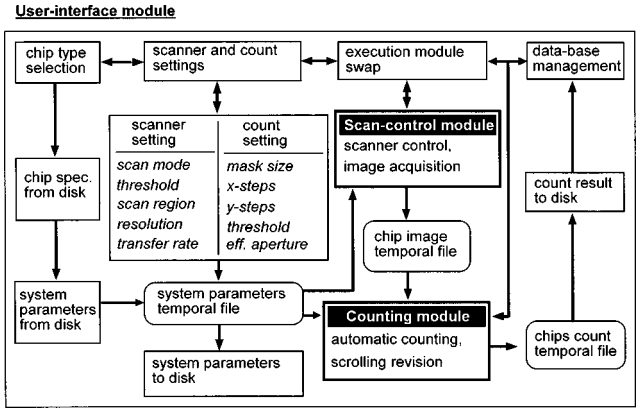

Fig. 8 Program architecture of the presented chip counting system.

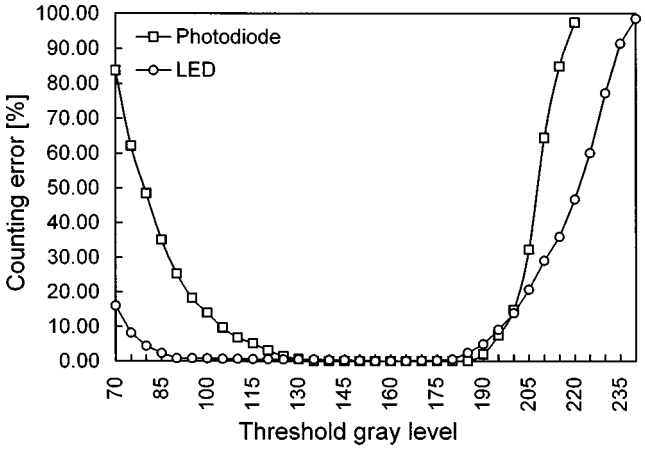

Fig. 9 Dependence of counting error on the chosen binary threshold level.

Hence, directly revising the defined parameters according to a counting result is feasible at the very beginning of calibration.

The mask method does not require complete separation between neighboring chips. As long as certain parts of the clearance grid exist, normal chip position can be detected easily with a mask matrix of appropriate size and jumping steps. Therefore this method has the advantage of allowing reasonable imperfections in the grabbed binary image. The decision to choose correct operation parameters, such as resolution, mask size, and motion distance can be made by an unskilled operator referring to the calibration information on the screen.

4 System Implementation

One additional advantage in utilizing a commercial scanner as the image input device for our purpose is that industrial TWAIN standards have been established for image pickup.[7] Hence any brand of scanner can be selected without considering compatibility. Such an advantage is not provided by a custom-designed system except at the additional cost of writing a special program.

To ease the task of software implementation, the system is divided into two modules: scanner control and counting. The former, which is provided by the vendor with the machine, is used to set up the scan mode, gray-level threshold, scan zone, resolution, and image conversion speed for optimal image quality.[8] The latter module is used for chip identification and enumeration. To have the abilities of high-speed counting and serially execution of the two modules, the data stored by the scan module are first transferred into a temporary image RAM file to enable the count module to open freely for the counting operation. In this way, the existing scanner driver can be fully used without any slight modification.

For a practical chip counting system, a user interface module having an easy-to-operate data bank must be established and connected externally for convenient storage, querying, revision, and other management functions.[9] Hence users can automatically load the predetermined parameters by selecting the chip type to be counted, swapping the scanning and counting modules, and storing the results in a databank. The entire system configuration is shown in Fig. 8 for reference.

The system adopted for this study comprises a PC and a commercial low-cost scanner of 600-dpi resolution. Both are readily available in regular electronics shops.

The operational cycle time is from 25 s for large dice to 40 s for small LEDs. Hence it requires roughly 22 sets to handle a production run of 2 billion pieces per month of LED with a 16-h operation day. The price paid is negligible with such a low-cost system ($\sim$\$30,000 for 22 sets) in comparison to a custom-designed system, which amounts to over half a million dollars.

5 Experimental Results and Discussions

As mentioned, precise selection of the binary threshold level is not required for the die counting operation. Figure 9 shows the dependence of count error on the chosen threshold. One observes that there is a range allowed for each type of dice with negligible error. Here for large photodiode dice ($\sim 120\times 120$ mil^2) it is about 20% of the full-scale (135 to 185), and for smaller LED dice ($\sim 10\times 10$ mil^2), about 4% (155 to 165). To obtain a better decision on threshold value during the calibration, a grabbed graphic image is first expanded to 256 full gray scale for 0.5 to 99.5% range of its maximal intensity. Recalibration is necessary only when the light intensity has observable variation after extended operation. This may last for 2000 to 3000 h, about 50% of the life of a fluorescent lamp.

The numbers of good dice on some tested samples were counted by the mask method with manual reviews as the references. Table 1 shows the results of the study on two different device sizes produced in a local foundry supporting this research, each with different tilt angles and image resolutions. Since the imaging scan time, which takes 5 s for each cycle remains unchanged, the time consumed was not counted in the table.

For smaller LED chips of 10×10 mil^2, scanning with 600-dpi resolution provides the best image for counting. The mask method spends 31 s to count 6785 dice on a tape without significant error (-0.03%) in the result. If the scan resolution is lowered to 400 dpi, then the LED image size reduces to a value slightly less than 16 pixels. We then found that the mask method is not applicable, since this program defines a minimal mask size of 4×4.

Table 1 Experimental results with different conditions.

Specimen	Scanning Conditions		Counting Results			Mask Conditions		
	Tilt (deg)	Resol. (dpi)	Count	Error (%)	Time (s)	M_x, M_y (pixels)	S_x, S_y=1 (pixels)	A_x, A_y (pixels)
LED 6785 good dice								
P_d=10 mils, P_c=10 mils	0	600	6783	−0.03	31	4	11	10
	10	600	6783	−0.03	31	4	11	10
	20	600	6783	−0.03	31	4	11	10
	30	600	6782	−0.04	31	4	11	10
	45	600	6780	−0.07	31	4	11	10
Photodiode, 603 good dice								
P_d=120 mils, P_c=10 mils	0	100	603	0.00	7	8	13	12
	0	150	603	0.00	10	12	20	19
	0	200	603	0.00	15	16	27	26
	10	100	603	0.00	7	8	13	12
	10	150	603	0.00	10	12	20	19
	10	200	603	0.00	15	16	27	26
	20	100	603	0.00	7	8	13	12
	20	150	603	0.00	10	12	20	19
	20	200	603	0.00	15	16	27	26
	30	100	602	−0.02	7	8	13	12
	30	150	603	0.00	10	12	20	19
	30	200	603	0.00	15	16	27	26
	45	100	602	−0.02	7	8	13	12
	45	150	603	0.00	10	12	20	19
	45	200	603	0.00	15	16	27	26

For photodiodes or power transistors having a much larger size, resolution should be reduced for demand speed. At 100-dpi resolution, the die clearance and the ink marks are both preserved in the obtained images. This method gives excellent results with no observable errors at the highest counting speed.

Errors increased slightly for high tilting die arrays, especially for a small-sized LED, which is probably due to the effect of the size of the mask. Referring to Table 1, the tilting effect appears at an angle larger than 30 deg for both the LED and photodiode. These large degrees of tilt can be avoided easily with automatic machine alignment. Nevertheless, although the largest error occurred in 45-deg-tilt cases, this was deemed tolerable by the chip manufacturer that supported this project.

Unlike a microscope camera system, the space above a scanner is completely available. Hence, incorporating an automatic loading-and-transferring stage to the chip counting system can be achieved easily without the upper space limitation. Any commercialized sheet transfer equipment thus can be adopted directly for the system.

6 Conclusion

The die counting system described in this paper demonstrated practical speed and accuracy. The cost and performance advantages are such that the conventional CCD systems cannot compete. With this system, the price of counting discrete devices is reduced to almost nothing and tremendous savings can be realized at a foundry.

The system is being used on the product line of the factory supporting this study. Although the function of this system is very specific, it should be useful for a variety of semiconductor components of similar features in the modern electronic industry. The modified scanner can also be applied to any object with a smooth and shiny surface.

Acknowledgment

This study is supported by the National Science Council of the Republic of China under project contract no. NSC-85-2215-E-009-040. Thanks also to Opto-Tech Corporation at the Science-Based Industrial Park in Hsinchu for providing the facilities and samples to complete this study.

References

1. B. E. Dom and V. Brecher, ''Recent advances in the automatic inspection of integrated circuits for pattern defects,'' *Mach. Vis. Appl.* **8**, 5–19 (1995).
2. N. Wittels and S. H. Zisk, ''Lighting design for industrial machine vision,'' in *Optics Illumination and Image Sensing for Machine Vision, Proc. SPIE* **728**, 47–56 (1986).
3. H. E. Schroeder, ''Practical illumination concept and technique for machine vision applications,'' in *Proc. Robots 8th Conf.* Vol. 14, pp. 24–43, Robotics International of SME (1984).
4. S. X. Godber and M. Robinson, ''Machine vision using line-scan sensors,'' in *Machine Vision Applications, Architectures, and System Integration, Proc. SPIE* **1823**, 114–130 (1993).
5. R. P. Kruger and W. B. Thompson, ''A technical and economic assessment of computer vision for industrial inspection and robotic assembly,'' *Proc. IEEE* **69**(12), 1524–1538 (1981).
6. B. H. Khalaj, H. Aghajan, A. Paulraj, and T. Kailath, ''Defect inspection of periodic patterns with low-order distortions,'' in *Machine Vision Applications in Industrial Inspection, Proc. SPIE* **2183**, 13–19 (1994).

7. TWAIN Working Group, *TWAIN White Paper*, TWAIN, San Jose, CA (1996).
8. Microtek Corporation, *Microtek Scanner Software Development Tools Programmer's Guide*, Microtek Corporation Ltd., Taiwan (1993).
9. F. M. Waltz, ''User interfaces for automated visual inspection systems,'' in *Machine Vision Systems Integration, SPIE* **CR36**, 105–137 (1991).

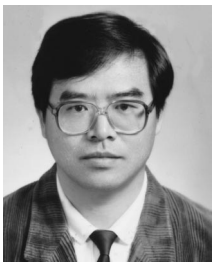

Tzong-Sheng Lee received his BS in physics from National Central University of Taiwan in 1980 and his MS in physics from National Tsing Hua University in 1984 and joined the Chung San Institute of Science and Technology, Tao Yuan, Taiwan, working on electro-optical system design and IR system simulations. He is currently a PhD candidate at the Institute of Electro-Optical Engineering of National Chiao Tung University studying machine vision applications.

Jin-Shown Shie is currently a professor with the Institute of Electro-Optical Engineering of National Chiao Tung University. He earned his BSEE from National Cheng Kung University, Taiwan, in 1965, his MSEE from National Chiao Tung University, Taiwan, in 1968, and his PhD in materials science from the State University of New York, Stony Brook. For the last 20 years, Dr. Shie has been working on photodetection technologies, from devices to application systems, and is a consultant to local industry in these fields. His present major research is in microsystem technology, especially in the fabrication of an uncooled focal-plane-array-type IR imager.